BIOMIRROR

A Structure-Based Drug Design Approach for the Identification of Novel Selective Cyclooxygenase-2 Inhibitors using Resveratrol Analogues as Lead Molecules

[a] Clarissa Caruana *,

[a] Claire Shoemake

[a] Department of Pharmacy, Faculty of Medicine and Surgery, University of Malta, MALTA.

ARTICLE INFO

ABSTRACT

Therapeutic areas for selective cyclooxygenase-2 inhibitors include inflammatory conditions and cancer. A study has demonstrated that hydroxylated analogues of resveratrol, which is found in red wine, inhibit cyclooxygenase-2 selectively. This study aimed to design *in silico* novel selective cyclooxygenase-2 inhibitors using two of these resveratrol analogues, namely 3,3',4',5-tetrahydroxystilbene and 3,3',4,4',5,5'-hexahydroxystilbene, as molecular templates. Two hundred molecules were generated *de novo* from each of these analogues. The binding affinities (pKd) of the novel molecules ranged from 9.70 to 10.00. In total, 10% of the molecules were compliant with Lipinski Rules, and hence, were orally bioavailable. The Lipinski Rules compliant molecules with high affinities can be included in libraries of selective cyclooxygenase-2 inhibitors to be used in high-throughput screening.

Introduction:

Cyclooxygenase (COX) isoenzymes catalyse the synthesis of prostanoids, namely prostaglandins, prostacyclin and thromboxane A_2[1]. COX-1 is constitutively expressed in most tissues of the body[1] and is mainly responsible for the production of prostaglandins involved in homeostatic processes, including the conservation of gastric mucosal integrity and renal function[2]. COX-2 is mostly induced and is the source of prostaglandins which promote fever, pain and inflammation[1].

Corresponding author: Clarissa Caruana *

E-mail address: clarissacaruana91@gmail.com

COX-2 is also over-expressed in several tumours and has oncogenic effects[3]. It is associated with tumour promotion, angiogenesis, metastasis and inhibition of apoptosis[4]. Selective inhibitors of COX-2 are chemopreventive, and they also sensitise tumour cells to the effects of chemotherapy or radiotherapy when used as adjuvant agents[3]. However, the duration of intake of COX-2 inhibitors is limited by the increased risk of cardiovascular thrombotic events, including myocardial infarction[5]. Therefore, COX-2 is a viable target for the design of selective COX-2 inhibitors having potential utility in the management of cancer and with an improved cardiovascular safety profile.

Products from natural sources can be used as lead compounds in the process of drug design. A study by Murias *et al.*[6] showed that hydroxylated analogues of resveratrol inhibit COX-2 selectively. Two of these analogues, namely 3,3',4',5-tetrahydroxystilbene and 3,3',4,4',5,5'-hexahydroxystilbene, are highly selective, with the latter being even more selective than the marketed selective COX-2 inhibitor, celecoxib[6]. This study aimed to design and optimise a series of selective COX-2 inhibitors which possess a high affinity for COX-2 and oral bioavailability, using 3,3',4',5-tetrahydroxystilbene and 3,3',4,4',5,5'-hexahydroxystilbene as molecular templates.

Method & Materials:

X-ray crystallographic deposition 3LN1[7] (Fig.1) was selected from the Protein Data Bank[9]. The deposition described the bound co-ordinates of the selective COX-2 inhibitor celecoxib with COX-2. COX-2 was crystallised as a tetramer, with each of the four chains bound to celecoxib. The 3D co-ordinates were read into Sybyl®-X v.1.2[10] and the deposition was simplified in order to reduce computer intensiveness in subsequent stages of the design process. Simplification was carried out via the removal of three *holo*-chains, namely A, C and D. This was followed by the removal of moieties, which were not considered critical to binding, from the remaining chain B. Water molecules were also removed. The result was a monomer of COX-2, chain B, bound to celecoxib (Fig. 2).

Figure 1. X-ray crystallographic deposition 3LN1, generated using Accelrys Discovery Studio® v.4.0[8]
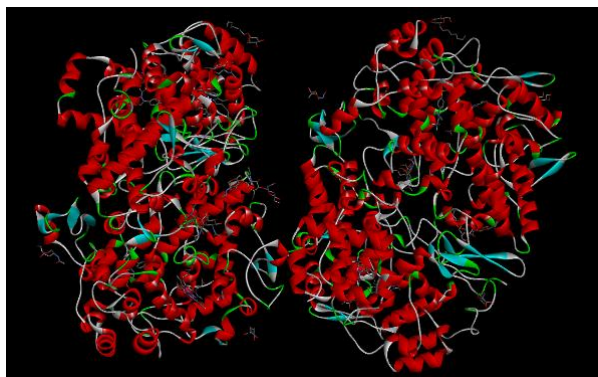

Figure 2. Celecoxib bound in the binding pocket of chain B, generated using Accelrys Discovery Studio® v.4.0[8]
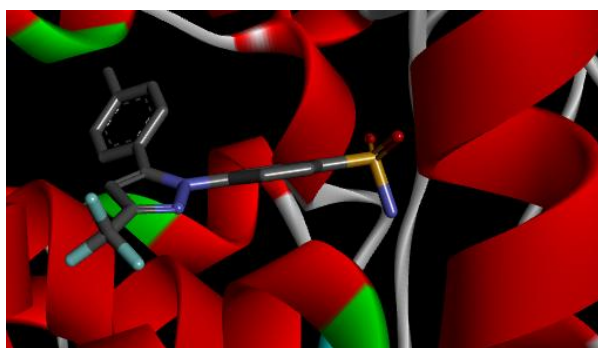

Using Sybyl®-X v.1.2[10], celecoxib was extracted with preserved co-ordinates from the ligand binding pocket (LBP) of COX-2, and saved in MOL2 format (Fig.3). The resultant *apo*-monomer was saved in PDB format. Both celecoxib and chain B were read into X-Score® v.1.3[11]and the Ligand Binding Affinity (LBA) (pKd) of celecoxib for COX-2 was calculated.

Figure 3. Celecoxib extracted from the COX-2 LBP, generated using Accelrys Discovery Studio® v.4.0[8]
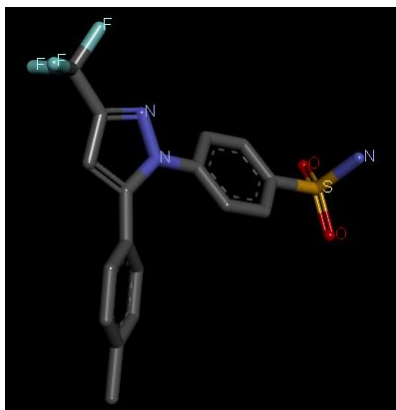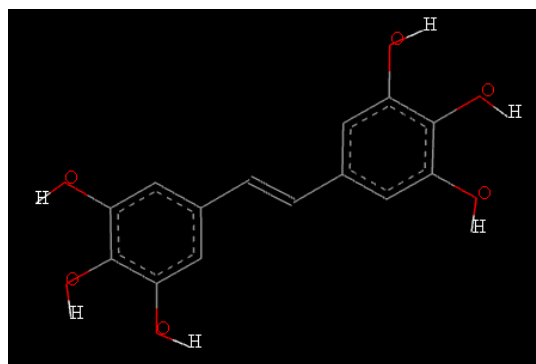

The resveratrol analogues 3,3',4',5-tetrahydroxystilbene and 3,3',4,4',5,5'-hexahydroxystilbene (Figs. 4-5) were sketched in Sybyl®-X v.1.2[10]and saved in MOL2 format.

Figure 4. Structure of 3,3',4',5-tetrahydroxystilbene,generated using Accelrys Discovery Studio® v.4.0[8]
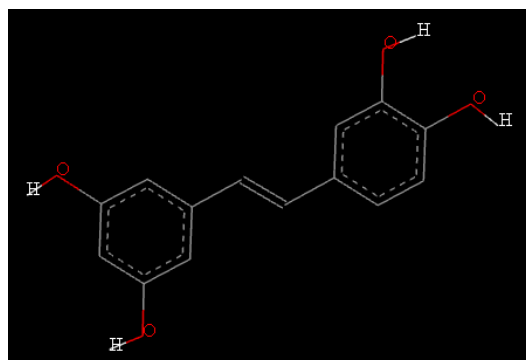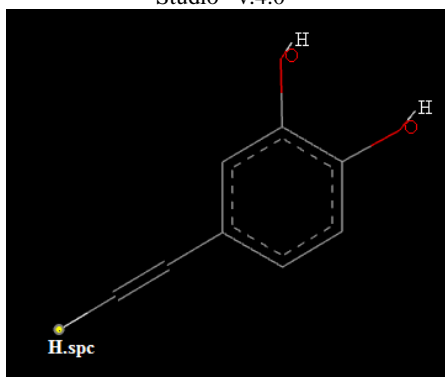

Figure 5. Structure of 3,3',4,4',5,5'-hexahydroxystilbene,generated using Accelrys Discovery Studio® v.4.0[8]


The resveratrol analogues were docked into the COX-2 LBP via Sybyl®-X v.1.2[10] using celecoxib in MOL2 format as a template. Conformational analysis was carried out and the twenty binding conformers having the highest affinities for COX-2 were selected. Each conformer was exported in MOL2 format.

Each binding conformer was read into X-Score® v.1.3[11] and its LBA (pKd) for COX-2 was quantified. The Ligand Binding Energy (LBE) (kcal mol^{-1}) of each conformer was calculated using Sybyl®-X v.1.2[10]. Graphs of LBA (pKd) and LBE (kcal mol^{-1}) against binding conformer number were plotted for each resveratrol analogue. The conformer exhibiting the optimal combination of high LBA (pKd) and low LBE (kcal mol^{-1}) was identified from the graph for each analogue. These two conformers were imported in Sybyl®-X v.1.2[10] for editing. Editing involved the removal of a benzene ring from each conformer, followed by the addition of a growing site via an atom type modification from a carbon atom to H.spc atom. This resulted in the formation of a seed structure, for each of the two optimal binding conformers (Figs 6-7), which was saved in MOL2 format.

Figure 6. Structure of seed derived from 3,3',4',5-tetrahydroxystilbene, generated using Accelrys Discovery Studio® v.4.0[8]

Figure7. Structure of seed derived from 3,3',4,4',5,5'-hexahydroxystilbene,generated using Accelrys Discovery Studio® v.4.0[8]
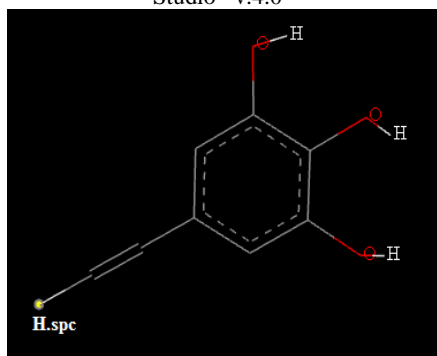
LigBuilder® v.1.2[12]was used for the *in silico* construction of novel molecules. LigBuilder® v.1.2[12] consisted of three modules, namely the POCKET module which analysed the LBP, the GROW module via which molecular growth occurred at the designated growing site, and the PROCESS module which generated the novel molecules.

Firstly, the parameter file for the POCKET module was edited, selecting Chain B as the receptor and the extracted celecoxib as the ligand. The POCKET module was then allowed to run. The parameter file for the GROW module was then edited. Each seed structure was used as an input file in the GROW module. The output files of the POCKET module, namely the atom file, which consisted of the atoms making up the LBP, and the grid file, which comprised the grids within the LBP, were also selected as input files. The GROW module was run twice, one time for each seed structure.

The ligand_collection_file, which resulted from the GROW module, was subsequently used in the PROCESS module. Two hundred novel molecules and an index file were created for each seed structure. The index file contained the family number, molecular formula, molecular weight, calculated logP and binding score (pKd) of each novel molecule.

The novel molecules were filtered according to LBA and Lipinski Rules[13]compliance criteria. The molecules which satisfied the criteria in terms of molecular weight and logP had their numbers of hydrogen bond acceptors and hydrogen bond donors calculated in Accelrys Draw®v.4.1[14] to establish whether they complied with all of the Lipinski Rules[13] criteria.

Results:

The LBA (p*K*d) of celecoxib was 7.40. This was used as a baseline against which the affinities (p*K*d) of the novel generated molecules were subsequently compared.

The twenty binding conformers of 3,3',4',5-tetrahydroxystilbene and 3,3',4,4',5,5'-hexahydroxystilbene are shown superimposed onto each other in Figures 8 and 9, respectively. The graph of LBA (p*K*d) and LBE (kcal mol^{-1}) against conformer number plotted for 3,3',4',5-tetrahydroxystilbene is displayed in Figure 10 and that plotted for 3,3',4,4',5,5'-hexahydroxystilbene is displayed in Figure 11. For each resveratrol analogue, the best binding conformer identified from the graph was the one having the highest peak distance between LBA (p*K*d) and LBE (kcal mol^{-1}), on the premise that this would combine high affinity with molecular stability.

Figure 8. Binding conformers of 3,3',4',5-tetrahydroxystilbene, generated using Accelrys Discovery Studio® v.4.0[8]. The optimal conformer is highlighted in yellow
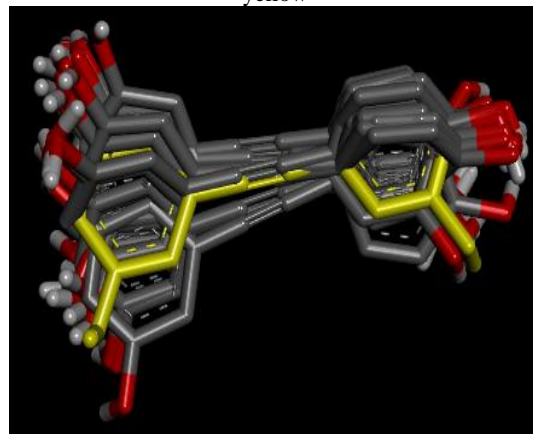

Figure 9. Binding conformers of 3,3',4,4',5,5'-hexahydroxystilbene, generated using Accelrys Discovery Studio® v.4.0[8]. The optimal conformer is highlighted in yellow
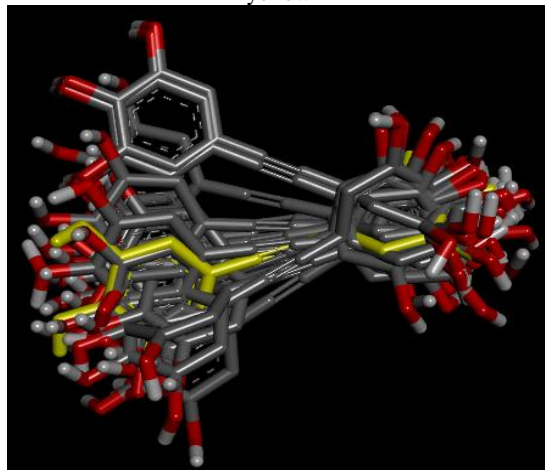
Figure 10. Graph of LBA (p*K*d) and LBE (kcal mol^{-1}) against conformer number for 3,3',4',5-tetrahydroxystilbene. The best conformer is encircled in green
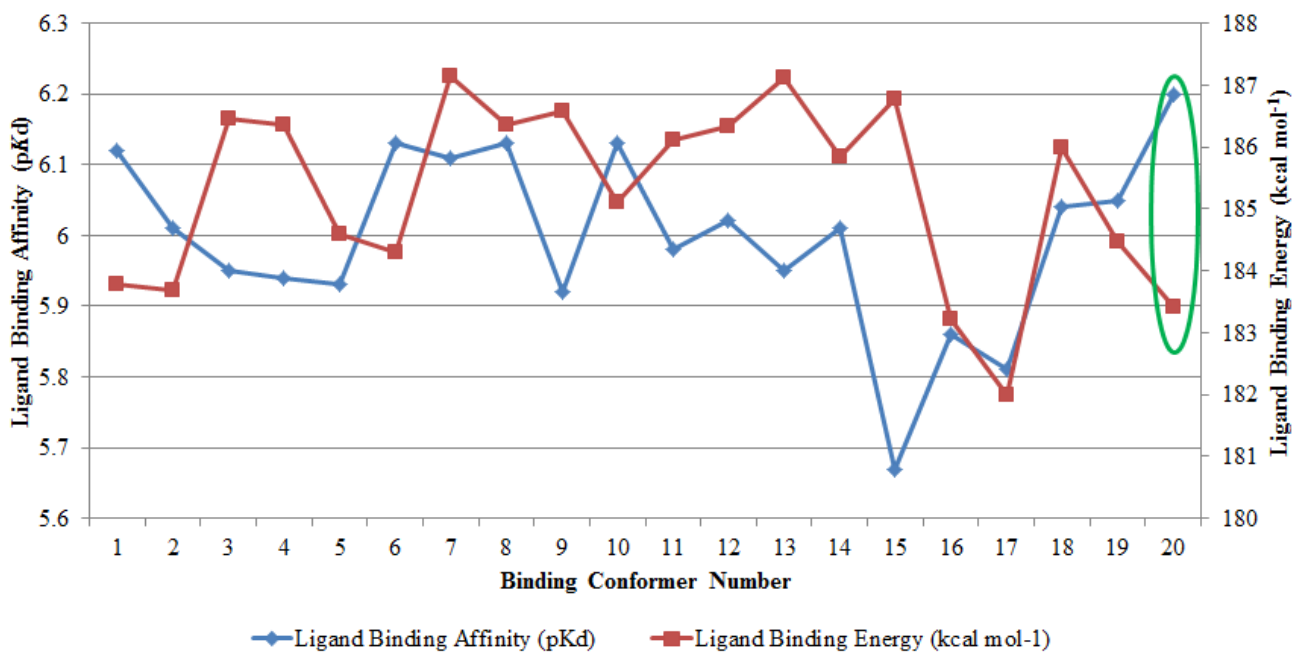

Figure 11. Graph of LBA (p*K*d) and LBE (kcal mol^{-1}) against conformer number for 3,3',4,4',5,5'-hexahydroxystilbene. The best conformer is encircled in green.
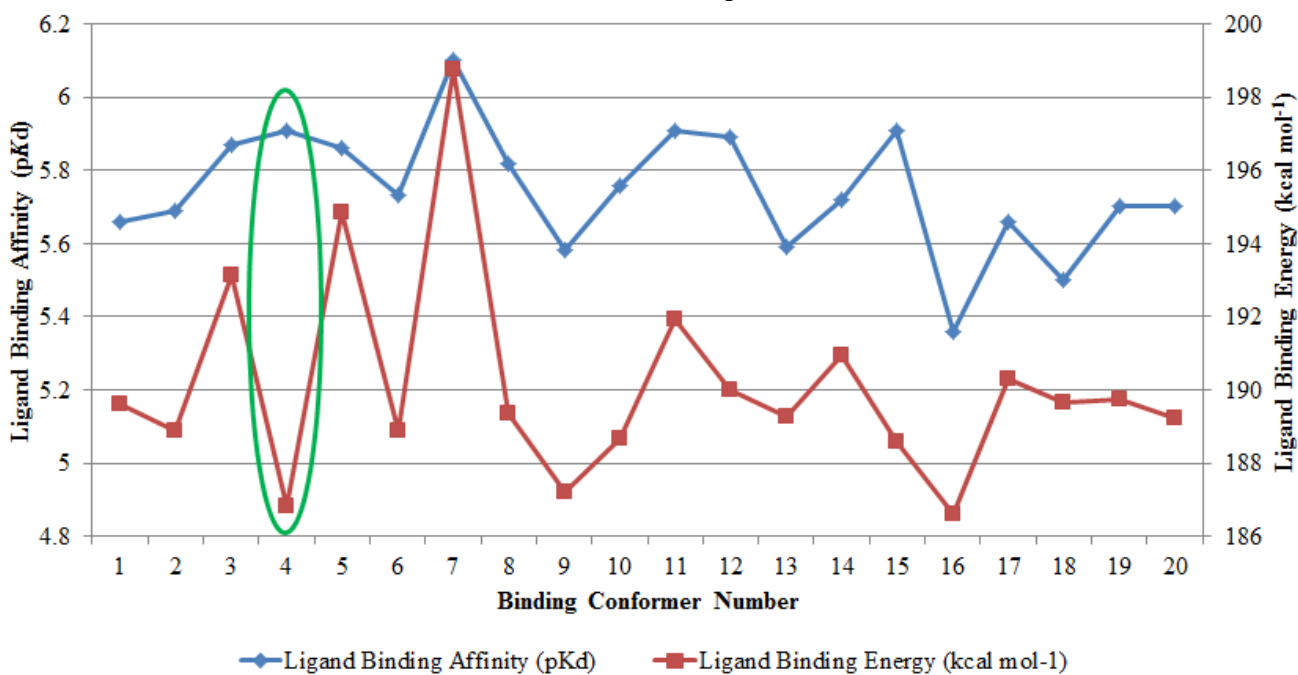
When the POCKET module within LigBuilder® v.1.2[12] was run, a key_site.pdb file and a pharmacophore.pdb file were derived. The key_site.pdb file represented the key binding sites (Fig.12) within the LBP of COX-2, whilst the pharmacophore.pdb file represented the pharmacophore model (Fig. 13) for COX-2.

Figure 12. Key interaction sites within COX-2, generated using Accelrys Discovery Studio® v.4.0[8]. Hydrogen bond donor grids are displayed in blue, hydrogen bond acceptor grids in red and hydrophobic grids in grey
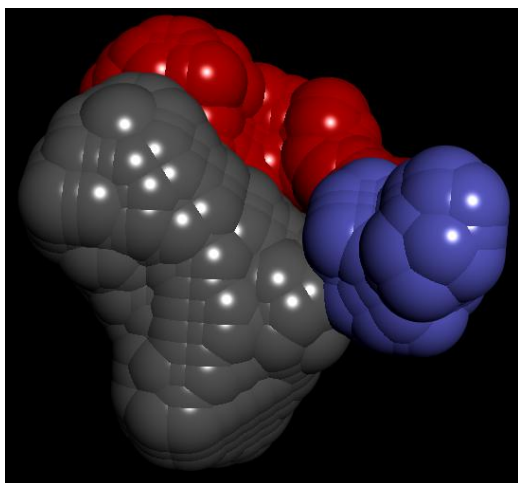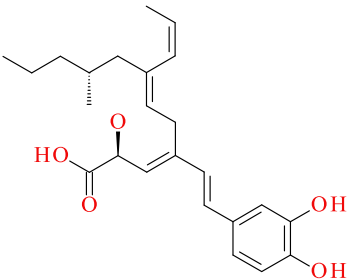

Two hundred molecules were created *de novo* for each resveratrol analogue. The LBAs (pKd) of the novel molecules generated from the seed structure of 3,3',4',5-tetrahydroxystilbene ranged from 9.73 to 10.00, whilst the affinities (pKd) of those derived from the seed structure of 3,3',4,4',5,5'-hexahydroxystilbene ranged from 9.70 to 10.00, higher than that of celecoxib (pKd 7.40).

Figure 13. Pharmacophore model for COX-2, generated using Accelrys Discovery Studio® v.4.0[8]. Hydrogen bond donor grids are displayed in blue, hydrogen bond acceptor grids in red and hydrophobic grids in grey
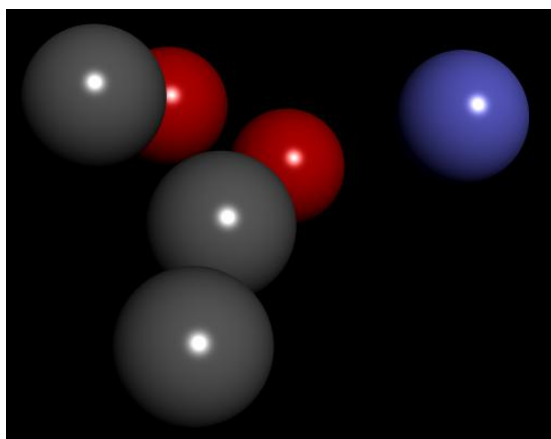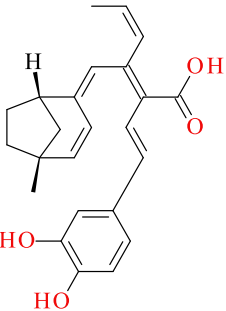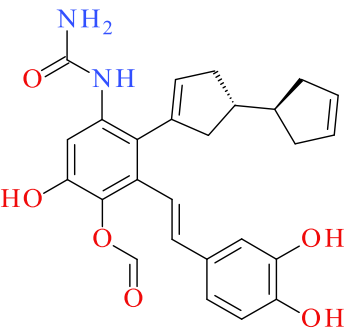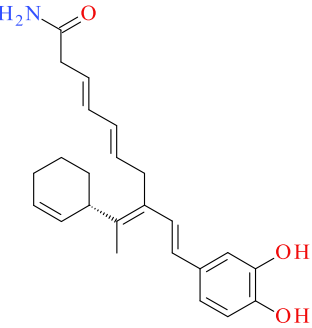

Lipinski Rules[13] state that drugs may be poorly absorbed by the body if the molecular weight is greater than 500, the logP is greater than 5, there are more than 10 hydrogen bond acceptors and there are more than 5 hydrogen bond donors. Twenty out of the two hundred novel molecules generated from the seed of 3,3',4',5-tetrahydroxystilbene, as well as twenty out of the two hundred molecules generated from the seed of 3,3',4,4',5,5'-hexahydroxystilbene, were compliant with Lipinski Rules[13]. The structures and properties of the Lipinski Rules[13] compliant molecules which have the highest LBA (pKd) values from their respective families are presented in Tables 1 and 2.
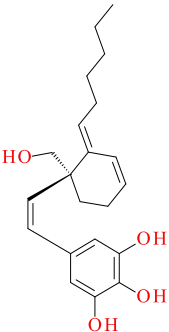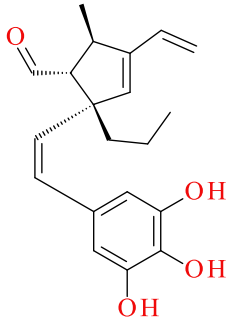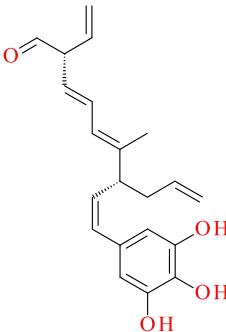
Table 1. Properties and structures of the Lipinski rules compliant molecules, having the highest pKd values, generated from the seed structure of 3,3',4',5-tetrahydroxystilbene. The structures were generated using Accelrys Draw® v.4.1[14]

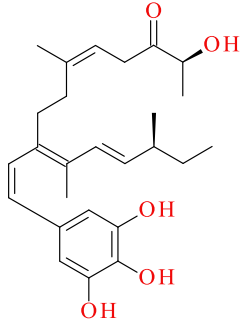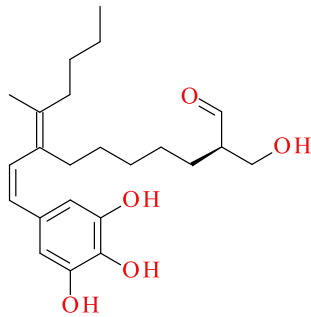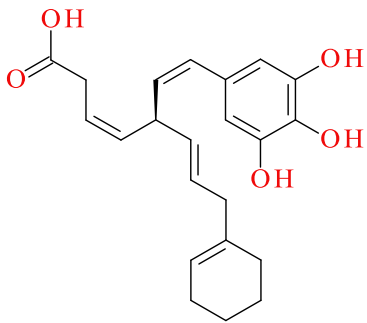| Family Number	LBA (pKd)	Molecular Weight	LogP	Number of Hydrogen Bond Acceptors	Number of Hydrogen Bond Donors	Structure
2	9.97	335	4.65	4	3	
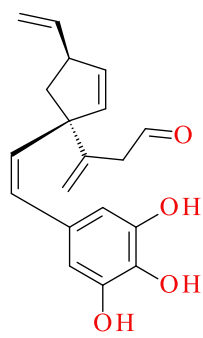
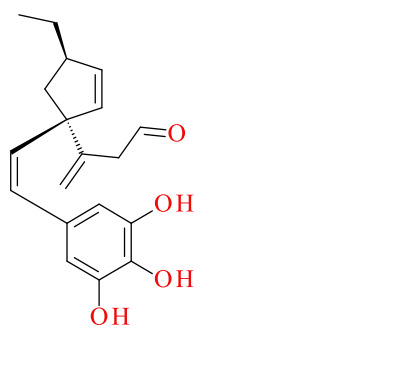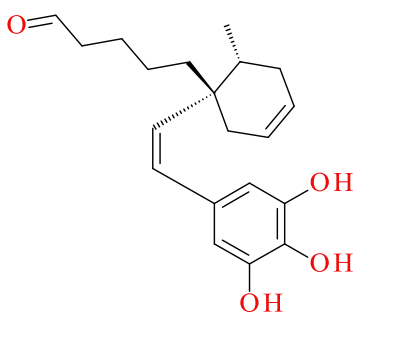| 3	10.00	394	4.96	5	4	
4	9.99	372	5.00	4	3	
7	9.86	457	4.45	6	5	
10	9.85	374	4.58	3	3	

BIOMIRROR

Table 2. Properties and structures of the Lipinski rules compliant molecules, having the highest pKd values, generated from the seed structure of 3,3',4,4',5,5'-hexahydroxystilbene. The structures were generated using Accelrys Draw® v.4.1[14]

Family Number	LBA (pKd)	Molecular Weight	LogP	Number of Hydrogen Bond Acceptors	Number of Hydrogen Bond Donors	Structure
1	9.84	340	4.95	4	4	
2	9.98	324	4.92	4	3	
4	9.74	336	4.74	4	3	

5	9.89	424	5.00	5	4	
6	9.85	386	4.94	5	4	
8	9.97	366	4.92	5	4	
9	9.82	308	4.56	4	3	

9	9.82	310	4.82	4	3	
11	9.87	326	4.98	4	3	

Figure 14. Structure of molecule number 16, generated using Accelrys Discovery Studio® v.4.0[8]
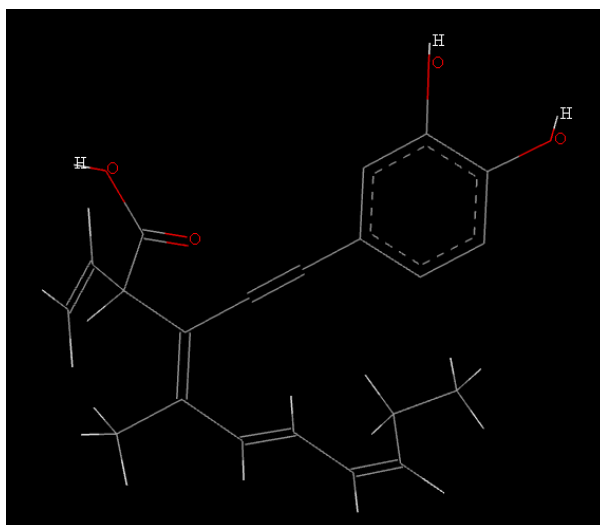

Discussion:

The pharmacophores of the families which comprised Lipinski Rules[13] compliant molecules, along with the binding affinities (pKd) of the molecules, were analysed to determine whether the addition or removal of a moiety at a particular *locus* resulted in an increase or loss of affinity.

The following observations were made for the Lipinski rules[13] compliant molecules constructed from the seed of 3,3',4',5-tetrahydroxystilbene:

1. Molecule number 16 (Fig. 14) had the highest affinity (pKd 9.97) within family number 2. A carboxyl group, at the *locus* encircled in Figure 15, took part in hydrogen bonding with Tyr[341] and Arg[106], and also formed an electrostatic interaction with Arg[106] (Fig. 16). At this *locus* in molecule number 89 (Fig.17), which had the lowest affinity (pKd 9.74) within the family, two aromatic rings were instead present and no hydrogen bonding or electrostatic interactions with Tyr[341] and Arg[106] were formed (Fig.18).
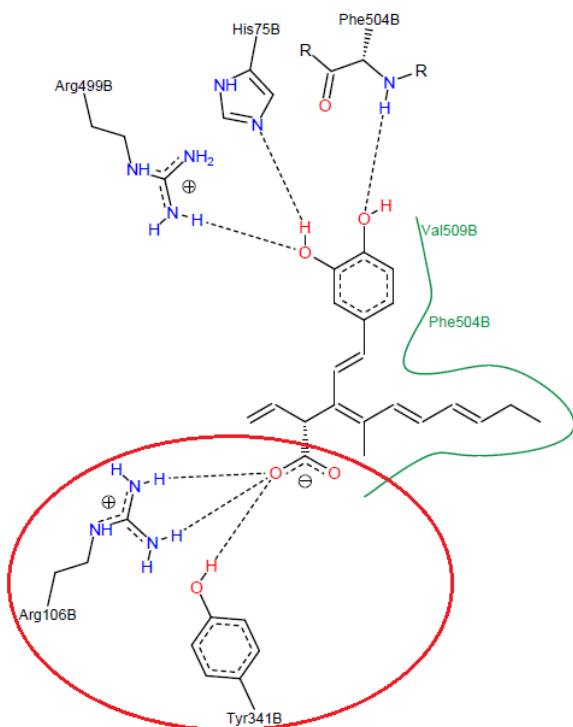
Figure 15. Pharmacophore of family number 2, generated using Accelrys Discovery Studio® v.4.0[8]. The *locus* at which differences in moieties may have resulted in differences in affinity is encircled in green
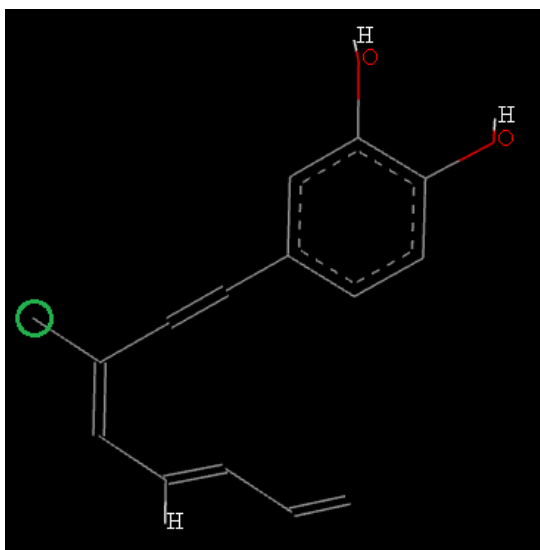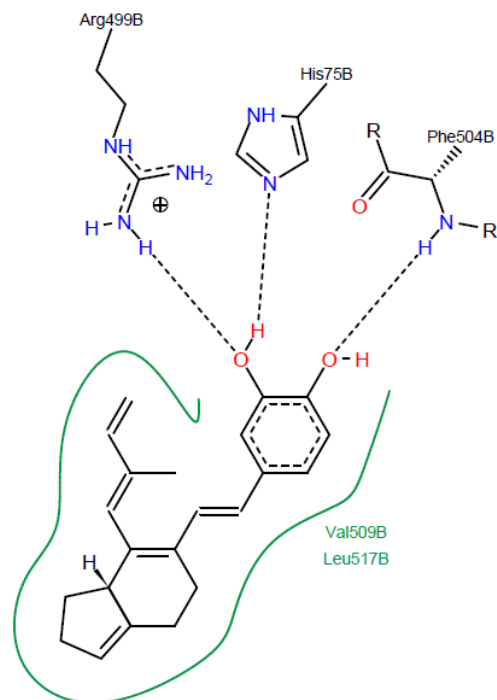

Figure 16. Interactions of molecule number 16 within LBP of COX-2, generated using PoseView[15]. The interactions with Arg[106] and Tyr[341] are encircled in red.

Figure 17. Structure of molecule number 89, generated using Accelrys Discovery Studio® v.4.0[8].
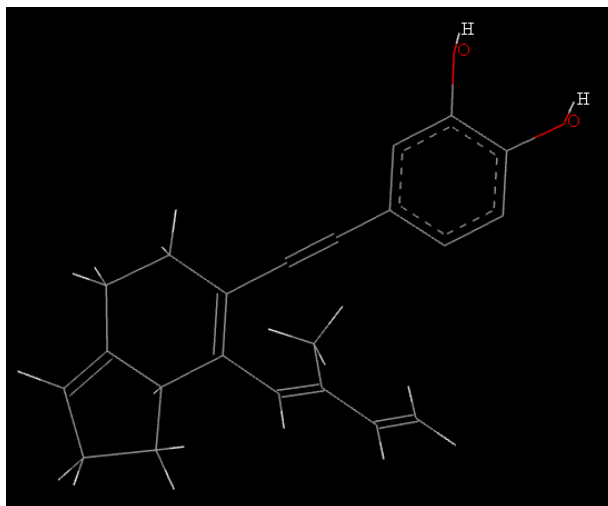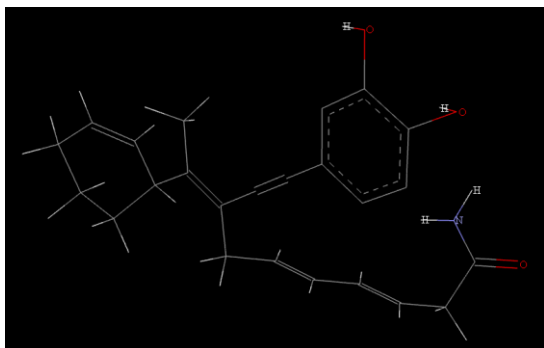

Figure 18. Interactions of molecule number 89 within LBP of COX-2, generated using PoseView[15]


2. Molecule number 185 (Fig. 19) had the highest affinity (p*K*d 9.85) within family number 10. In molecule number 185, an amide moiety originated from the *locus* encircled in Figure 20, but was absent in molecule number 190 (Fig. 21), which had the lowest affinity (p*K*d 9.75) within this family. The amide moiety formed a hydrogen bond with Met[508] (Fig.22). Molecule number 190 did not form a hydrogen bond with Met (Fig. 23).

**Figure 19.** Structure of molecule number 185, generated using Accelrys Discovery Studio® v.4.0[8]

Figure 20. Pharmacophore of family number 10, generated using Accelrys Discovery Studio® v.4.0[8]. The *locus* at which differences in moieties may have resulted in differences in affinity is encircled in green
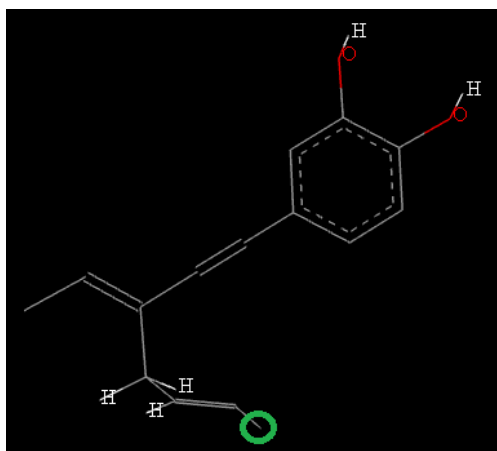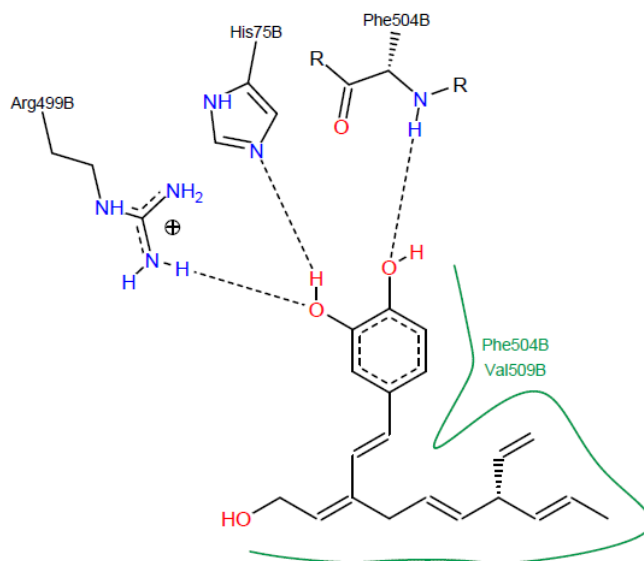

Figure 21. Structure of molecule number 190, generated using Accelrys Discovery Studio® v.4.0[8]
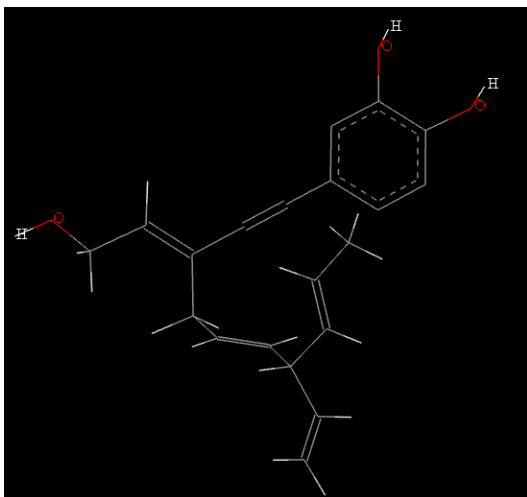
Figure 22. Interactions of molecule number 185 within LBP of COX-2, generated using PoseView[15]. The hydrogen bond with Met[508] is encircled in red
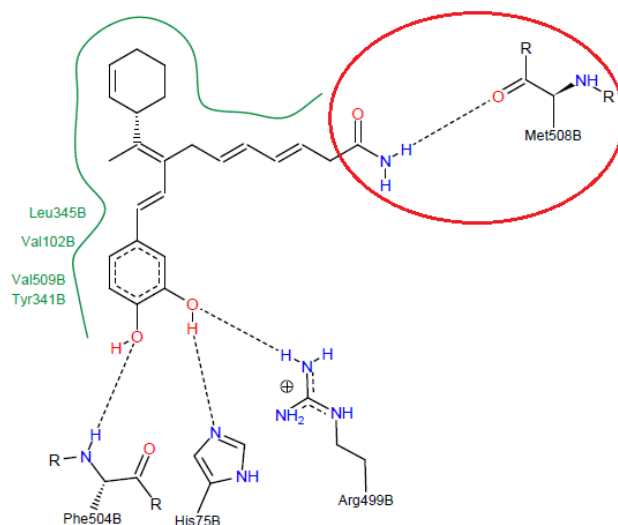
Figure 23. Interactions of molecule number 190 within LBP of COX-2, generated using PoseView[15]


For the Lipinski Rules[13] compliant molecules derived from the seed of 3,3',4,4',5,5'-hexahydroxystilbene, the following was determined:

1. In molecule number 26 (Fig. 24), which had the highest affinity (pKd 9.84) in family number 1, an aromatic ring was present at the *locus* encircled in Figure 25. This ring was absent in molecule number 45 (Fig. 26) which had the lowest affinity (pKd 9.71) in this family. The

aromatic ring could be the reason as to why molecule number 26 made hydrophobic contact with another amino acid, namely Ser[339], compared to molecule number 45 (Figs. 27-28).
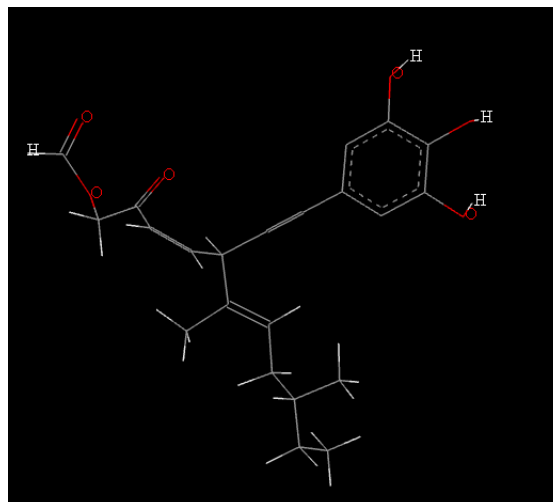
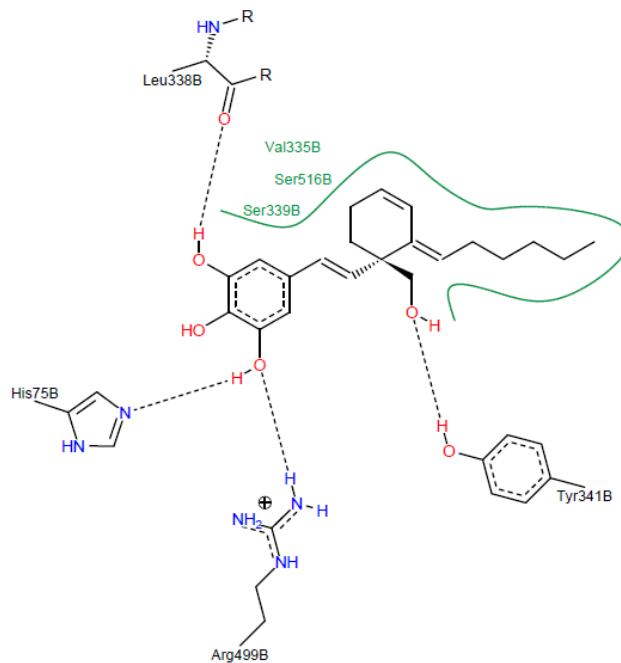**Figure 24.** Structure of molecule number 26, generated using Accelrys Discovery Studio® v.4.0[8]
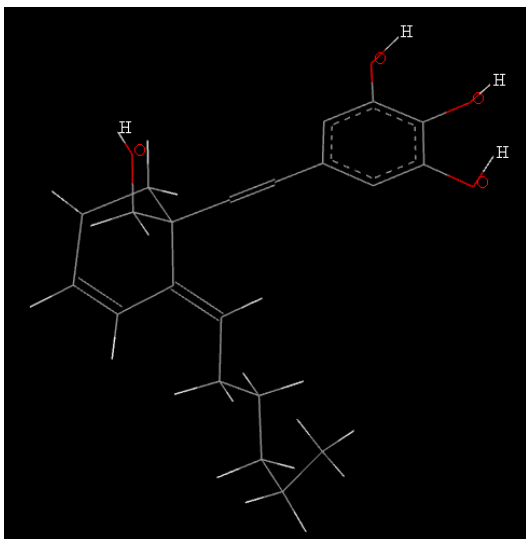
Figure 25. Pharmacophore of family number 1, generated using Accelrys Discovery Studio® v.4.0[8]. The *locus* at which differences in moieties may have resulted in differences in affinity is encircled in green
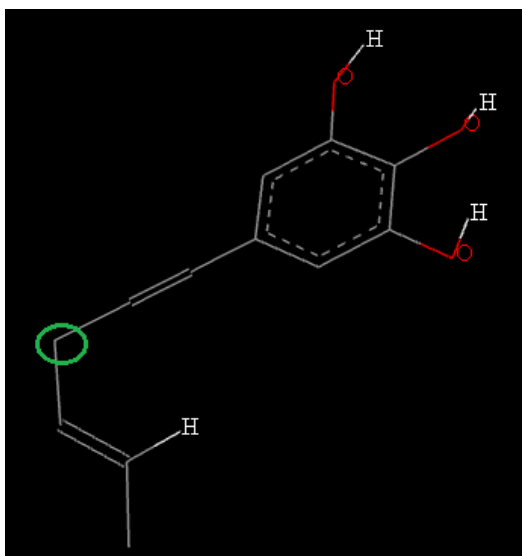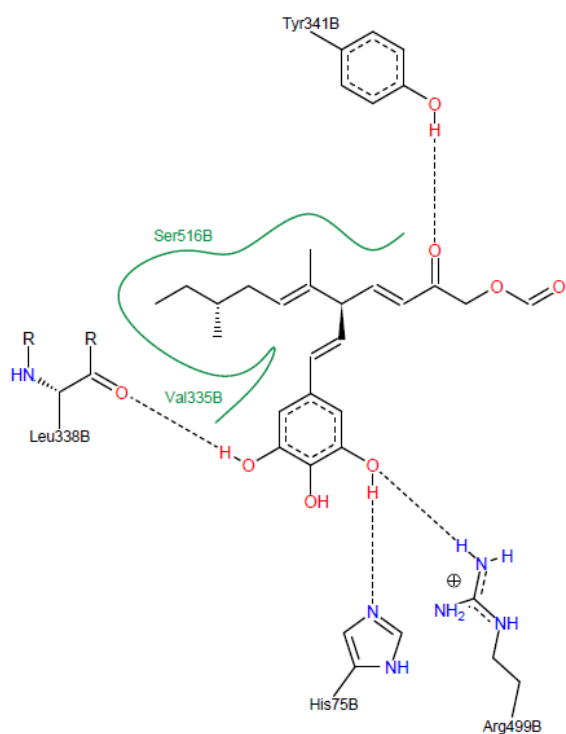

**Figure 26.** Structure of molecule number 45, generated using Accelrys Discovery Studio® v.4.0[8]

Figure 27. Interactions of molecule number 26 within LBP of COX-2, generated using PoseView[15]
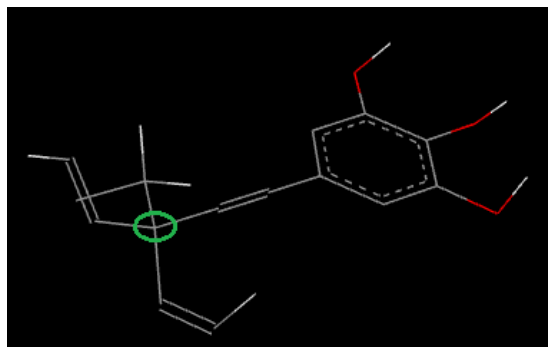
Figure 28. Interactions of molecule number 45 within LBP of COX-2, generated using PoseView[15]

Figure 30. Structure of molecule number 173, generated using Accelrys Discovery Studio® v.4.0[8]
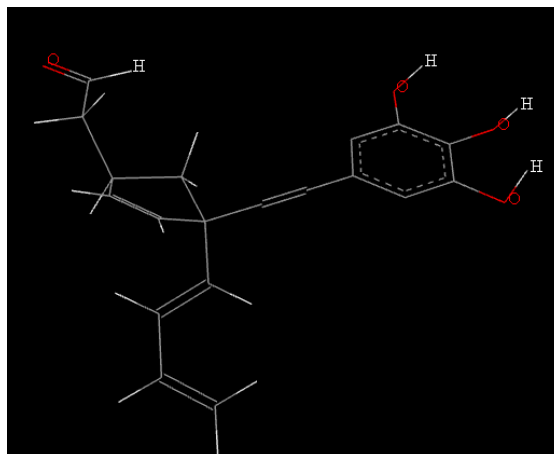

Figure 31. Pharmacophore of family number 9, generated using Accelrys Discovery Studio® v.4.0[8]. The *locus* at which differences in moieties may have resulted in differences in affinity is encircled in green

2. For family number 9, molecule number 169 (Fig. 29) had the highest affinity (pKd 9.82), and molecule number 173 (Fig. 30) had the lowest affinity (pKd 9.73). Both molecules had an aromatic ring at the *locus* encircled in Figure 31. In molecule number 169, the side chain of the ring consisted of an ethyl group, whilst in molecule number 173 it comprised an aldehyde moiety. The ethyl group may have resulted in molecule number 169 being involved in two more hydrophobic interactions, namely with Tyr[341] and Leu[345], than molecule number 173 (Figs. 32-33).

Figure 29. Structure of molecule number 169, generated using Accelrys Discovery Studio® v.4.0[8]
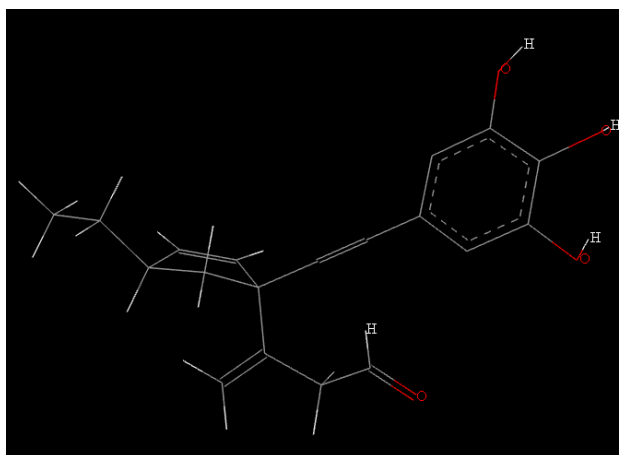
Figure 32. Interactions of molecule number 169 within LBP of COX-2, generated using PoseView[15]
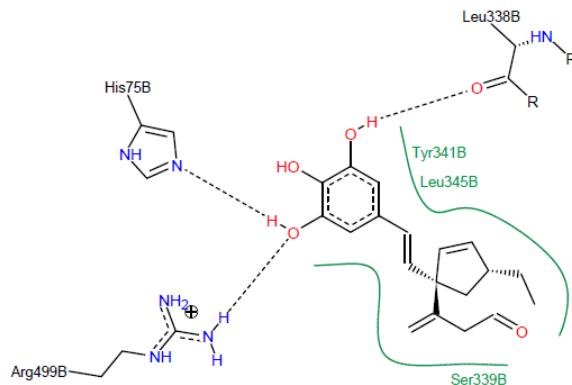
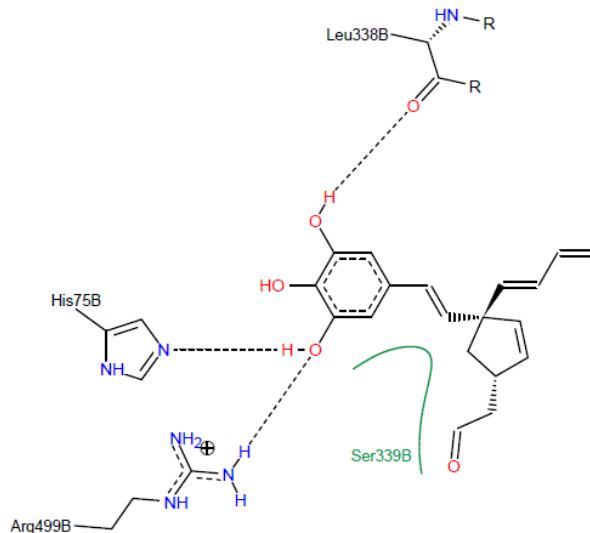**Figure 33.** Interactions of molecule number 173 within LBP of COX-2, generated using PoseView[15]

Conclusion:

This study identified novel *in silico* generated selective COX-2 inhibitors which have both high LBA (p*K*d) for the COX-2 receptor, and which, being Lipinski Rules[13] compliant, are orally bioavailable. These can be included in libraries of molecules which selectively inhibit COX-2 to be used in high-throughput screening.

Reference:

1. Smith WL, DeWitt DL, Garavito RM (2000) Cyclooxygenases: structural, cellular, and molecular biology. Annu Rev Biochem 69: 145-182.

2. van Ryn J, Trummlitz G, Pairet M (2000) COX-2 selectivity and inflammatory processes. Curr Med Chem 7(11): 1145-1161.

3. Rizzo MT (2011) Cyclooxygenase-2 in oncogenesis. Clin Chim Acta 412(9-10): 671-687.

4. Ghosh N, Chaki R, Mandal V, Mandal SC (2010) COX-2 as a target for cancer chemotherapy. Pharmacol Rep 62(2): 233-244.

5. Fanelli A, Romualdi P, Vigano' R, Lora Aprile P, Gensini G, Fanelli G (2013) Non-selective non-steroidal anti-inflammatory drugs (NSAIDs) and cardiovascular risk. Acta Biomed 84(1): 5-11.

6. Murias M, Handler N, Erker T, Pleban K, Ecker G, Saiko P, et al. (2004) Resveratrol analogues as selective cyclooxygenase-2 inhibitors: synthesis and structure-activity relationship. Bioorg Med Chem 12(21): 5571-5578.

7. Wang JL, Limburg D, Graneto MJ, Springer J, Hamper JR, Liao S et al. (2010) The novel benzopyran class of selective cyclooxygenase-2 inhibitors. Part 2: the second clinical candidate having a shorter and favorable human half-life. Bioorg.Med.Chem.Lett 20(23): 7159-7163.

8. Accelrys Software Inc., Discovery Studio, Release 4.0, San Diego, CA, USA.

9. Bernstein FC, Koetzle TF, Williams GJ, Meyer EF, Brice MD, Rodgers JR, et al. (1977) The Protein Data Bank: a computer-based archival file for macromolecular structures. J Mol Biol 112(3): 535-542.

10. SYBYL-X 1.2, Tripos International, 1699 South Hanley Rd., St. Louis, Missouri, 63144, USA.

11. Wang R, Lai L, Wang S (2002) Further Development and Validation of Empirical Scoring Functions for Structure-Based Binding Affinity Prediction.J. Comput.-Aided Mol. Des 16: 11-26.

12. Wang R, Gao Y, Lai L (2000) LigBuilder: A Multi-Purpose Program for Structure-Based Drug Design. J Mol Model 6(7-8): 498-516.

13. Lipinski CA, Lombardo F, Dominy BW, Feeney PJ (1997) Experimental and computational approaches to estimate solubility and permeability in drug discovery and development settings. Adv Drug Deliv Rev 23(1-3): 3-25.

14. Accelrys Software Inc., Draw, Release 4.1, San Diego, CA, USA.

15. Stierand K, Maass PC, Rarey M (2006) Molecular complexes at a glance: automated generation of two-dimensional complex diagrams. Bioinformatics 22(14): 1710-1716.